

Linking preferred orientation of shale minerals to their elasticity

Venkatesh Anantharamu* and Lev Vernik, Ikon Science Americas Inc., Houston, Texas, USA.

SUMMARY

The elastic velocity and anisotropy of shales are significantly affected by the orientation distribution of clay minerals including mica. A lot of research has been done on elastic properties of clay and clay aggregates with varying degree of the platelet preferred orientation. However, our understanding regarding the properties are still limited. In this study, we use both experimental and empirical rock physics models (RPM) for conventional shale to constrain elastic properties of muscovite and illite. The orientation distribution data from the published literature is used to relate the maximum platelet pole density to the median orientation angle. We then propose a heuristic approach to model anisotropic elastic moduli and P- and S-wave velocities of zero-porosity clay (matrix) aggregates as a function of the median orientation angle.

INTRODUCTION

Shales are phyllosilicate mineral-rich heterogeneous rocks that can be recognized as a source rock, cap rock and a reservoir. The anisotropy of shales can be a combined effect of clay platelet preferred orientation (Kaarsberg, 1959; Hornby et al., 1994; Sayers, 1994), kerogen, and crack alignment at various scales (Vernik, 1997). The results of multiple laboratory experiments show that the anisotropy of shales can be approximated as transverse isotropy (TI) with a rotational symmetry axis normal to bedding plane.

Preferred orientation of clay platelets normally forms during mechanical compaction with some recrystallization at the advanced stages of diagenesis (Wenk, 2007). The process of recrystallization can either enhance or reduce the alignment depending on the stress history. The degree of clay mineral preferred orientation can be expressed as the maximum pole density (MPD) in multiples of a random distribution - m.r.d. (Wenk, 1985), in which higher values reflect higher degrees of preferred orientation and the values can go until infinity for the perfect bedding-plane alignment. The orientation distribution (OD) of clay minerals along with mica significantly affects the anisotropic elastic moduli of TI shales. The information on elastic properties of clay minerals is very crucial in doing rock physics modeling and seismic interpretation, and pore pressure prediction.

The clay minerals and mica are among the main constituents of shales and their volume fraction ranges from 30-90% on the solid rock basis, i.e., independent of porosity (Vernik, 2016). Hence, the knowledge of elastic moduli and density of various clay minerals and mica are required for modeling purposes. Unfortunately, this knowledge is still rather limited because of the very fine-grained nature of their aggregates, so that no direct measurements can be performed.

Understanding the limitations, Katahara (1996) used the labo-

ratory measurements of mica (e.g., muscovite by Alexandrov and Ryzhova, 1961) to estimate the moduli of clay minerals such as illite which shares the structure and composition with muscovite. Several authors (Tosaya, 1982; Castagna et al., 1985; Han et al., 1986) relied on empirical relationship between velocity and porosity with clay content. Bayuk (2007) use a theoretical model to invert for elastic moduli. A more comprehensive study was presented by Louis et al. (2018), who used extensive X-ray goniometry measurements and XRD mineralogy analyses on the Kimmeridgian shales.

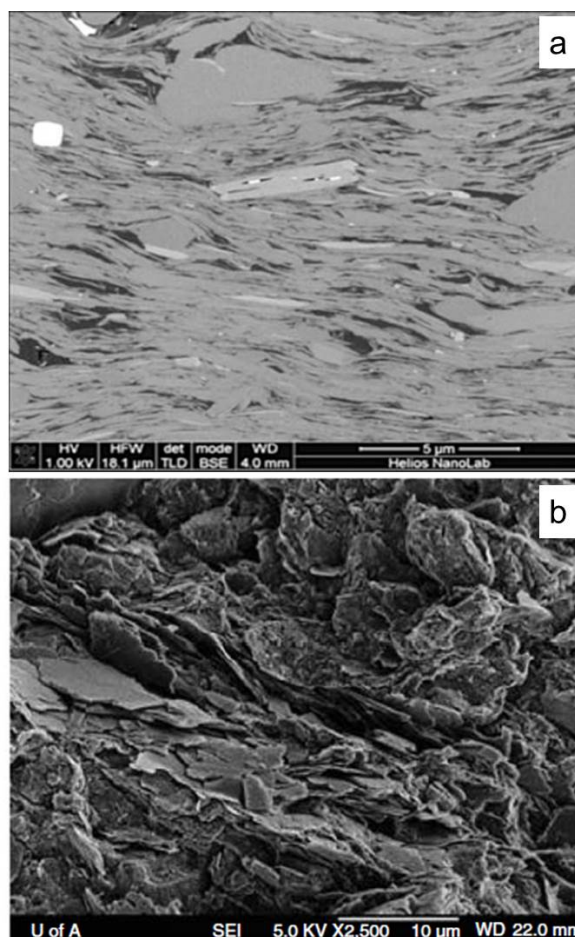


Figure 1: (a) SEM backscatter image of Woodford shale (porosity is less than 10%), which shows strong preferred orientation of illite-dominated clay platelets (MPD > 13 m.r.d., $V_{cl} = 0.34$). (b) SEM image of a shale subject to the maximum burial depth of 700 m with a porosity of about 36% and some minor preferred orientation of predominantly illite/smectite and kaolinite platelets ($V_{cl} = 0.63$); this shale presents an example of the quasi-isotropic clay aggregate with MPD ≈ 3 m.r.d.

In this paper, we use the clay platelet orientation distribution measurements using X-ray goniometry reported for shales

Clay mineral orientation

of different compaction and recrystallization by Wenk (2007, 2018), Day-Stirrat (2012), and Louis et al. (2018). The orientation strength refers to the basal planes (001) (or the poles to those planes) of mica and clay particles. In the process, we replace the maximum pole density (MPD in m.r.d.) value with the median orientation angle, τ . Figure 1 shows actual high resolution SEM images of the (1) highly compacted and diagenetically altered illite-rich shale with $V_{cl} = 0.34$ and the estimated MPD in the 12-20 m.r.d. range and (2) poorly compacted mud with $V_{cl} = 0.63$ and the MPD estimated at 3 ± 1 m.r.d.

The main objectives of this study are (1) to develop a simple function relating P- and S-wave velocity in zero-interparticle-porosity clay aggregates to the platelet orientation strength and, consequently, (2) to estimate elastic tensors of the most ubiquitous phyllosilicate constituents of muds and mudrocks, such as mica and illite-dominated shales to be used in sonic and seismic modeling and interpretation.

METHOD

The theoretical model to determine the elastic properties of composite polycrystalline minerals from the elastic properties of components can be approached in several ways. The isotropic composite of randomly-oriented TI particles (Watt, 1976) using Voigt and Reuss can be computed as follows:

$$K_v = \frac{1}{9}(4C_{11} + C_{33} + 4C_{13} - 4C_{66})$$

$$G_v = \frac{1}{30}(2C_{11} + 2C_{33} - 4C_{13} + 10C_{66} + 12C_{44}) \quad (1)$$

$$K_R = (2S_{11} + S_{33} + 4S_{13} + 2S_{12})$$

$$G_v = \frac{1}{30}(2C_{11} + 2C_{33} - 4C_{13} + 10C_{66} + 12C_{44}) \quad (2)$$

The relationships between the compliance and stiffness coefficients for TI medium (Fedorov, 1968) are as follows:

$$S_{11} = \frac{C_{11}C_{33} - C_{13}^2}{\Delta}$$

$$S_{33} = \frac{C_{11}^2 - C_{12}^2}{\Delta}$$

$$S_{13} = \frac{C_{13}(C_{12} - C_{11})}{\Delta} = -\frac{2C_{66}C_{13}}{\Delta}$$

$$S_{44} = \frac{1}{C_{44}}$$

$$S_{66} = \frac{1}{C_{66}}$$

$$S_{12} = \frac{C_{13}^2 - C_{12}C_{33}}{\Delta}$$

$$\Delta = 4C_{66}(C_{11}C_{33} - C_{13}^2 - C_{33}C_{66})$$

$$= 4C_{66}(C_{33}(C_{11} - C_{66} - C_{13}^2)) \quad (3)$$

The subscripts V and R denote the Voigt and Reuss averages, respectively. C_{ij} and S_{ij} are single crystal stiffness and compliance tensors, respectively, written in the Voigt contracted

notation. K and G denote bulk and shear moduli respectively, so from isotropic elasticity we can obtain the P-wave modulus $M = K + \frac{4}{3}G$. Finally, the Hills average (Hill, 1952) can be computed by taking an arithmetic average of the Voigt and Reuss moduli.

Orientation distribution function (ODF)

The simplest and, arguably the best fitting model for the pole density orientation data is given by the Owens-March function (Louis et al., 2018):

$$f(\alpha) = \frac{Z}{[Z^2 + \sin^2(\alpha)(1 - Z^2)^{3/2}]^2} \quad (4)$$

where α is the inclination angle away from the vertical axis and Z is the fitting parameter, which is reduced to $Z = \frac{1}{\sqrt{MPD}}$ when $\alpha = 0^\circ$.

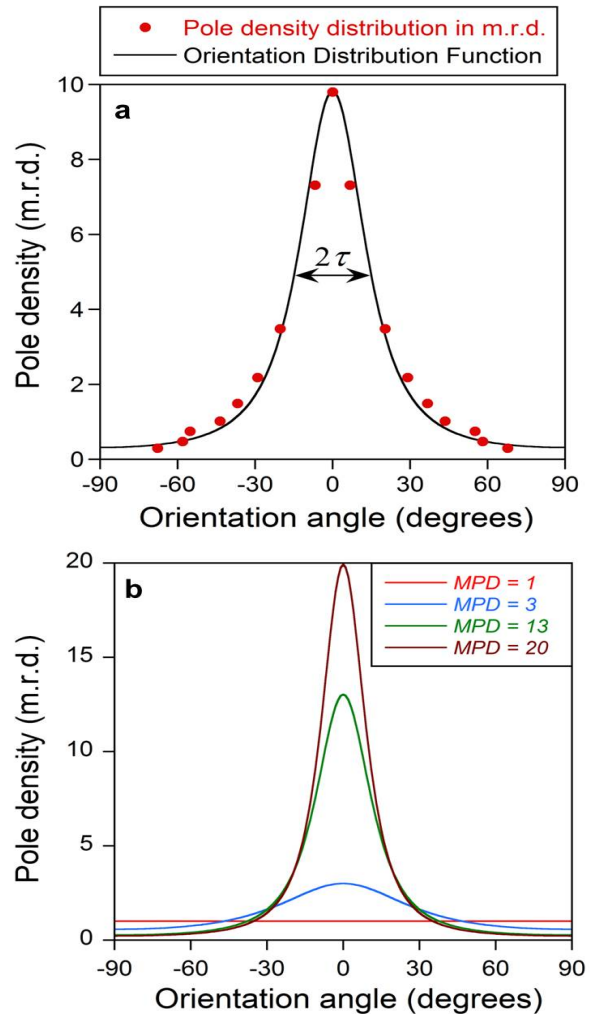


Figure 2: OD data on pole density of clay platelets with the best-fitting Owens-March ODFs superposed for (a) Cambrian shale, (b) the Owens-March ODFs with the MPD values of 1, 3, 13, and 20 m.r.d. Note that the blue line for MPD = 3.0 intersects the random orientation line (red) at -45 and 45.

Clay mineral orientation

The MPD is measured in m.r.d. units given in the logarithmic scale to describe the results of any X-ray goniometry-based pole density distribution data; therefore, the Owens-March ODF can be easily generated and compared to the experimental data. The OD data were digitized for the Kimmeridgian and Devonian shale samples (Louis et al., 2018), the illite-rich Cambrian shale (Wenk, 2007), and the Devonian slate (Wenk, 2018). The digitized data were fitted with the Owens-March ODF, which we will refer to as a Z-function henceforth. It can be seen in figure 2a that the Z-function fits the data reasonably well.

For the purposes of our modelling, instead of MPD, we replace it with alternative orientation strength parameter that can be referred to as the median orientation angle (τ), which is equal to the width of the ODF at half MPD. If an ODF is plotted over the angle range from -90 to 90 for completeness, the angle 2τ can be introduced as shown in Figure 2a. The relation between the MPD and τ can be seen in Figure 2b, where the ODFs with the MPD values of 1, 3, 13, and 20 are shown.

RESULTS

Muscovite

Muscovite is a phyllosilicate mineral from the group of micas. Its chemical composition is given by the formula: $KAl_2(AlSi_3)O_{10}(OH)_2$ (Rieder et al., 1998). The five independent C_{ij} tensor elements and the mineral density reported in (Vaughan and Guggenheim, 1986) are: $C_{11} = 181.0$ GPa, $C_{33} = 58.6$ GPa, $C_{44} = 16.5$ GPa, $C_{66} = 72.0$ GPa, and $\rho_m = 2.81 \pm 0.02$ g/cm³. Respective Thomsen TI parameters are: $\epsilon = 1.04$, $\gamma = 1.68$, $\delta = 0$. Most notably and quite symptomatic of the measurements uncertainty at 45 to the TI symmetry axis (e.g., Chichinina and Vernik, 2018), Vaughan and Guggenheim mention the uncertainties with C_{13} and δ in their experiments as well, so the plausible range for δ is 0-0.06, i.e., still positive.

From the Voigt and Reuss bounds for elastic moduli (equations 1 and 2) and the relations between compliance and stiffness coefficients of TI medium (equations 3) the isotropic moduli of the muscovite aggregate with random crystal orientation with zero porosity, and zero crack density can be computed. The results for the P-wave and shear moduli are $M_H = 104.7$ GPa, $G_H = 35.2$ GPa, respectively. The isotropic velocities are $V_P = 6.10$ km/s and $V_S = 3.54$ km/s and the ratio is $\frac{V_P}{V_S} = 1.723$. An ideal muscovite aggregate with perfect crystal alignment will mimic the tensor elements of the muscovite monocrystal. Therefore, we fix the end points of the bedding-normal and bedding-parallel stiffnesses in the modulus vs. DMO-angle space and seek a simple function that will describe the variations in terms of the median orientation angle τ or 2τ . We propose the elliptical functions $C_{ij} = f(2\tau)$, Figure 3 shows the experimental measurement-based anchor points at $2\tau = 0$ and the elliptical functions describing the variations in bedding-normal and bedding-parallel P- and S-wave velocities in muscovite aggregate with platelet alignment ranging from perfect to random. Equations 5 shows the the bedding-normal

and bedding-parallel velocities as a function of the preferred orientation of the highly anisotropic micas and clay mineral aggregates in shales.

$$\begin{aligned} V_P(0^\circ) &= \sqrt{\frac{C_{33} \cos^2(2\tau) + M_H \sin^2(2\tau)}{\rho_m}} \\ V_P(90^\circ) &= \sqrt{\frac{C_{11} \cos^2(2\tau) + M_H \sin^2(2\tau)}{\rho_m}} \\ V_S(0^\circ) &= \sqrt{\frac{C_{44} \cos^2(2\tau) + G_H \sin^2(2\tau)}{\rho_m}} \\ V_S(90^\circ) &= \sqrt{\frac{C_{66} \cos^2(2\tau) + G_H \sin^2(2\tau)}{\rho_m}} \end{aligned} \quad (5)$$

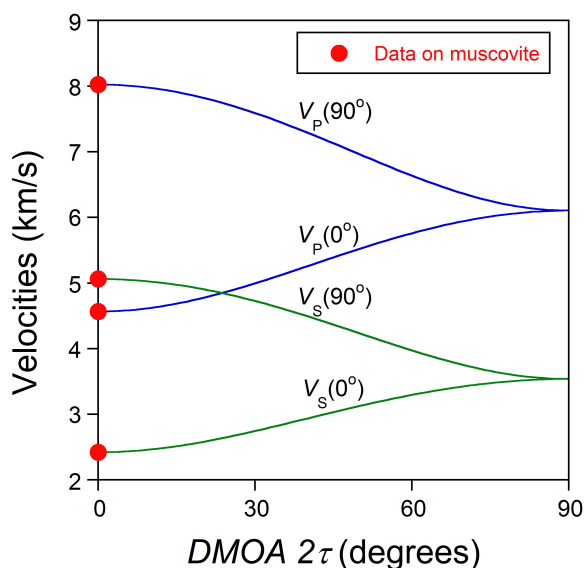


Figure 3: Bedding-normal and bedding-parallel velocities of P- and S-waves vs. the DMO angle 2τ for muscovite using the elliptical functions

Illite-rich clay

Illite is a common clay mineral with variable chemical composition that can be described by the following formula: $(KH_3O)(AlMgFe)_2(SiAl)_4O_{10}[(OH)_2(H_2O)]$ (Rieder et al., 1998). Although illite shares similar crystallographic structure with muscovite, its level of hydration is significantly greater. Moreover, illite has an additional chemically-bound hydroxyl (OH) and water H_2O^+ molecules, containing approximately 3% of physically-bound water H_2O^- in between its tetrahedral aluminosilicate sheets. This fact together with direct mineral density measurements for both dry (i.e., without H_2O) and fully hydrated illite reported by Edmundson and Raymer (1979) allowed Vernik (2016) to bracket its grain density at 2.64-2.70 g/cm³ averaging 2.67 g/cm³, i.e., 5% lower than that of muscovite.

From Louis et al. (2018) we find that the relationship between

Clay mineral orientation

the MPD and volume of illite-rich clay dominating the total clay fraction in their Kimmeridgian and Devonian shale samples is given by:

$$MPD = 10V_{cl} + 1.7 \quad (6)$$

where, V_{cl} is the volume fraction of clay on the solid rock basis. For $V_{cl} = 1$ equation 6 yields the MPD value of around 12 ± 1 . The width of the best-fitting Z-function at half MPD = 13 (e.g., Figure 2b), i.e., the double median orientation angle of the zero-porosity clay aggregate is $2\tau = 22^\circ$ in this low porosity shale. This implies a strong, but still not perfect preferred orientation of the illite-rich aggregates. Vernik and Kachanov (2010) and Vernik (2016) present a simple power-law RPM accounting for the bedding-normal P-wave velocity $V_P(0^\circ)$ and matrix density variation with porosity ϕ and bulk density in conventional shales (total organic carbon TOC < 1.5%). From the RPM we can estimate the following bedding-normal matrix moduli of illite-dominated clay aggregates at $V_{cl} = 1$: $C_{33} = 33.4$ GPa and $C_{44} = 8.5$ GPa.

Based on petrographic evidence it is reasonable to assume that these values refer to the median orientation angle of 11° ($2\tau = 22^\circ$). From these, we attempt to use these moduli and velocities as constraints to estimate the moduli of illite-rich clay aggregate at perfect platelet orientation, i.e., at $\tau = 0^\circ$. We notice that using these constraints on moduli at strong (but not perfect) preferred orientation and relatively low value of $2\tau < 25^\circ$ the range of educated guesses on $C_{33@2\tau=0}$ for the perfect platelet alignment with the bedding plane is rather limited. Moreover, the possible range can be further constrained if we assume that the ratio of C_{33} at the perfect crystal alignment to that at random one obtained for muscovite also applies to illite-rich clay aggregate, i.e., $\frac{C_{33@2\tau=0}}{M_H} \approx 0.56$. Figure 4 graphically illustrates that application of equations 5 for $C_{33}(2\tau)$ to match the illite moduli anchor points with this additional constraint recovers its value at $2\tau = 0^\circ$ of $C_{33@2\tau=0} = 30.0$ GPa. Even relaxing the assumption on the moduli ratio from exactly 0.56 to a looser range, the outcome for $C_{33@2\tau=0}$ may hardly exceed the 29.0-31.0 GPa range, i.e., the uncertainty in the $V_P(0^\circ)$ value of the perfectly aligned illite-rich clay composite is not expected to exceed 3%. If we make yet another, even though less substantiated, assumption that the anisotropy parameters of illite are the same as those for muscovite, we obtain the value of $C_{11@2\tau=0} = 92.4$ GPa for the perfect platelet alignment. Similarly, we can derive $C_{44@2\tau=0} = 7.34 \pm 0.3$ GPa and $C_{66@2\tau=0} = 32.0$ GPa.

To verify the accuracy of our assumptions and at least partially validate the results for the isotropic moduli of illite-dominated clay matrix composite, we back-calculate the moduli using the equations 1 and 2 to obtain $M_H = 53.1$ GPa and $G_H = 16$ GPa. These values are within 2% from those estimated from the moduli ratios across the range of orientations derived for muscovite.

The elastic moduli were also calculated for illite/smectite dominated clay composite but due to limitation of space, it is not presented here.

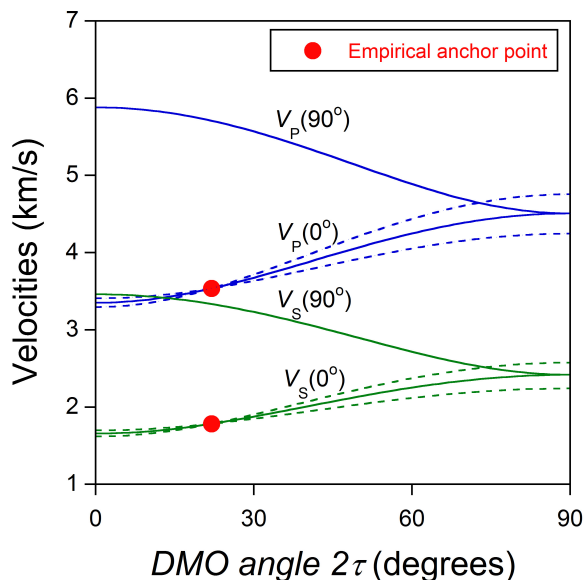


Figure 4: Bedding-normal and bedding-parallel velocities of P- and S-waves vs. the DMO angle 2τ for illite-dominated clay aggregate using the elliptical functions

CONCLUSIONS

The elastic properties of clay minerals are necessary for rock physics modeling of both conventional and unconventional shales. However, our knowledge of them is still limited and often controversial. Orientation distribution data can be related in a heuristic approach to model anisotropic elastic moduli and P- and S-wave velocities of zero-porosity clay (matrix) aggregates as a function of the median orientation angle. The zero-porosity mica and clay aggregates with perfect platelet alignment ($\tau = 0$) and dominated by illite should have the bedding-normal elastic moduli of $C_{33} = 30.0$ GPa, $C_{44} = 7.34$ GPa, and $\frac{V_P}{V_S}$ ratio of around 2.0. The respective moduli and mineral density of muscovite are significantly greater.

ACKNOWLEDGEMENTS

The authors would like to thank Ikon Science for support and permission to publish this study. Special thanks to Dr. Mark Sams, Dr. Simon Payne and Dr. Alan Mur for reviewing the manuscript and improving its quality.

REFERENCES

- Alexandrov, K. S., and T. V., Ryzhova, 1961, Elastic properties of rock forming minerals 2: Layered silicates: Bulletin USSR Academy of Science, Geophysics Series **11**, 871–875.
- Bayuk, I. O., M., Ammerman, and E. M., Chesnokov, 2007, Elastic moduli of anisotropic clay: *Geophysics*, **72**, no. 5, D107–D117, doi: <https://doi.org/10.1190/1.2757624>.
- Castagna, J. P., M. L., Batzle, and R. L., Eastwood, 1985, Relationships between compressional-wave and shear-wave velocities in clastic silicate rocks: *Geophysics*, **50**, 571–581, doi: <https://doi.org/10.1190/1.1441933>.
- Chichinina, T., and L., Vernik, 2018, Physical bounds on C13 and d for organic mudrocks: *Geophysics*, **83**, no. 5, A75–A79, doi: <https://doi.org/10.1190/geo2018-0035.1>.
- Day-Stürat, R. J., P. B., Flemings, A. C., Aplin, and B. A., van der Pluijm, 2012, The fabric of consolidation in Gulf of Mexico mudstones: *Marine Geology*, **295–298**, 77–85, doi: <https://doi.org/10.1016/j.margeo.2011.12.003>.
- Edmundson, H., and L. L., Raymer, 1979, Radioactive logging parameters for common minerals: *The Well Log Analyst*, **20**, 38–47.
- Fedorov, F. I., 1968, Theory of elastic waves in crystals: Plenum Press (originally in Russian, 1965, Nauka).
- Han, D. H., A., Nur, and D., Morgan, 1986, Effects of porosity and clay content on wave velocities in sandstones: *Geophysics*, **51**, 2093–2107, doi: <https://doi.org/10.1190/1.1442062>.
- Hill, R. W., 1952, The elastic behavior of a crystalline aggregate: *Proceedings of the Physical Society Section A London*, **65**, 349–354, doi: <https://doi.org/10.1088/0370-1298/65/5/307>.
- Hornby, B. E., L. M., Schwartz, and J. A., Hudson, 1994, Anisotropic effective-medium modeling of the elastic properties of shales: *Geophysics*, **59**, 1570–1583, doi: <https://doi.org/10.1190/1.1443546>.
- Kaarsberg, E. A., 1959, Introductory studies of natural and artificial argillaceous aggregates by sound-propagation and X-ray diffraction methods: *The Journal of Geology*, **67**, 447–472, doi: <https://doi.org/10.1086/626597>.
- Katahara, K., 1996, Clay mineral elastic properties: 66th Annual International Meeting, SEG, Expanded Abstracts, 1691–1694, doi: <https://doi.org/10.1190/1.1826454>.
- Louis, L., R., Day-Stürat, R., Hoffmann, N., Saxena, and A. M., Schleicher, 2018, Computation of effective elastic properties of clay from X-ray texture goniometry data: *Geophysics*, **83**, no. 5, MR245–MR261, doi: <https://doi.org/10.1190/geo2017-0581.1>.
- Rieder, M., G., Cavazzani, Y. S., D'Yakonov, V. A., Frank-Kamenetskii, G., Gottardi, S., Guggenheim, P. V., Koval, G., Müller, A. M. R., Neiva, E. W., Radaslovich, J.-L., Robert, F. P., Sassi, H., Takeda, Z., Weiss, and D. R., Wones, 1998, Nomenclature of the micas: *The Canadian Mineralogist*, **36**, 905–912.
- Sayers, C. M., 1994, The elastic anisotropy of shales: *Journal of Geophysical Research-Solid Earth*, **99**, 767–774, doi: <https://doi.org/10.1029/93JB02579>.
- Tosaya, C. A., 1982, Acoustical properties of clay-bearing rocks: Ph. D thesis, Stanford University.
- Vaughan, M. T., and S., Guggenheim, 1986, Elasticity of muscovite and its relationship to crystal structure: *Journal of Geophysical Research*, **91**, 4657–4665, doi: <https://doi.org/10.1029/JB091iB05p04657>.
- Vernik, L., 2016, Seismic petrophysics in quantitative interpretation, 2nd ed.: SEG.
- Vernik, L., and M., Kachanov, 2010, Modeling elastic properties of siliciclastic rocks: *Geophysics*, **75**, no. 6, E171–E182, doi: <https://doi.org/10.1190/1.3494031>.
- Vernik, L., and X., Liu, 1997, Velocity anisotropy in shales: A petrophysical study: *Geophysics*, **62**, 521–532, doi: <https://doi.org/10.1190/1.1444162>.
- Watt, J. P., G. F., Davies, and R. J., O'Connell, 1976, The elastic properties of composite media: *Reviews of Geophysics*, **14**, 541–563, doi: <https://doi.org/10.1029/RG014i004p00541>.
- Wenk, H., I., Lonardelli, H., Franz, K., Nihei, and S., Nakagawa, 2007, Preferred orientation and elastic anisotropy of illite-rich shale: *Geophysics*, **72**, no. 2, E69–E75, doi: <https://doi.org/10.1190/1.2432263>.
- Wenk, H. R., ed., 1985, Preferred orientation in deformed metal and rocks: Academic Press.
- Wenk, H. R., W., Kanitpanyacharoen, and Y., Ren, 2018, Slate — A new record for crystal preferred orientation: *Journal of Structural Geology*, **125**, 319–324 article in press, doi: <https://doi.org/10.1016/j.jsg.2017.12.009>.